THE ARCHIVE OF MECHANICAL ENGINEERING

Vol. LII 2005 Number 4

Key words: *fatigue crack growth, prediction models, aluminium alloys*

*MAŁGORZATA SKORUPA**), *TOMASZ MACHNIEWICZ**), *ANDRZEJ SKORUPA**)

THE NASGRO STRIP YIELD MODEL PREDICTIONS ON FATIGUE CRACK GROWTH FOR AIRCRAFT ALUMINIUM ALLOYS UNDER CONSTANT AMPLITUDE AND VARIABLE AMPLITUDE PROGRAMMED AND RANDOM LOADING

The strip yield model from the NASGRO computer software has been applied to predict fatigue crack growth in two different aircraft aluminium alloys under constant amplitude loading and programmed and random variable amplitude load histories. The computation options realized included either of the two different strip yield model implementations available in NASGRO and two types of the input material data description. The model performance has been evaluated based on comparisons between the predicted and observed results. It is concluded that altogether unsatisfactory prediction quality stems from an inadequate constraint factor conception incorporated in the NASGRO models.

1. Introduction

For a successful implementation of the damage tolerance philosophy to the design and in-service operation of structures subjected to fatigue loading it is crucial to have reliable crack growth prediction tools. Elber's [1] discovery of plasticity-induced crack closure and subsequent recognizing its utility in explaining such fatigue crack growth characteristics as the load interaction phenomena occurring under variable amplitude (VA) loading or the stress ratio (R) and thickness effects, stimulated a generation of crack growth prediction models which incorporated plasticity-induced crack closure. Among such concepts extensively reviewed elsewhere [2], the

*) *AGH University of Science and Technology, Al. Mickiewicza 30, 30-059 Kraków, Poland; E-mail: mskorupa@uci.agh.edu.pl*

so-called strip yield (SY) model based on the Dugdale conception of crack tip plasticity, but modified to allow forming a wedge of plastically deformed material on the surfaces of an advancing crack, remains a particularly versatile predictive tool convenient to use in the case of mode I fatigue crack growth under arbitrary VA loading histories.

According to the crack closure concept, the crack opening stress (S_{op}) in a current load cycle depends on the plastic deformations in the crack wake, which result from the loads experienced previously. With the SY model, all plastic deformation is confined within an infinitely thin strip located along the crack line and embedded in perfectly elastic material. The strip stresses and deformations are solved using numerical methods by considering compatibility conditions along the fictitious crack surface, Fig. 1. To this end, the plastic strip is divided into a number of bar elements. The elements in the plastic zone can carry both tensile and compressive stresses, whilst the broken elements in the crack wake can only undergo compressive stresses referred to as the contact stresses. The S_{op} level for a given load cycle is determined from the contact stress distribution at the minimum load.

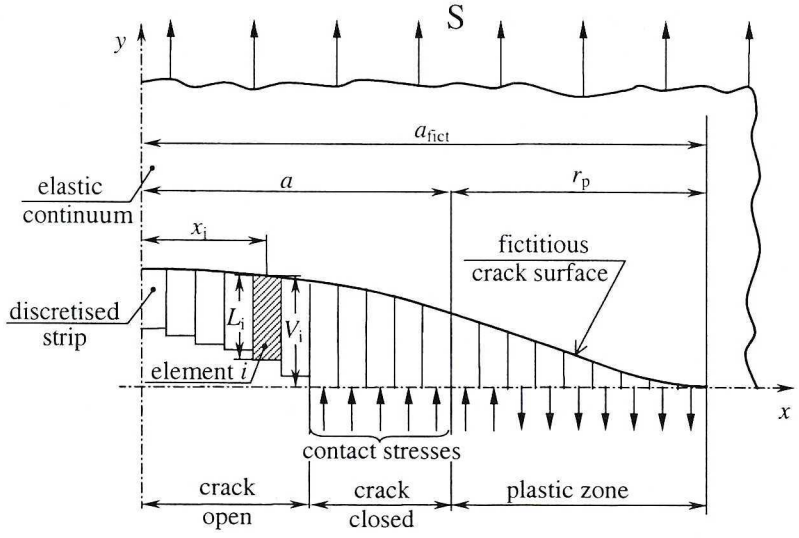

Fig. 1. Schematic illustration of the discretized plastic strip

A number of SY model implementations have been proposed, which differ in various respects. Typically, strip material is assumed to be rigid-perfectly plastic, e.g. [3], [4], or elastic-perfectly plastic, e.g. [5], but attempts to account for strain hardening have also been reported, e.g. [6], [7]. The S_{op} value can be computed either from the condition of equilibrium

between the stress intensity factor due to an applied stress increment (S_{op}-S_{min}) and the (artificial) stress intensity factor due to the contact stresses, as first proposed by Newman [3], or alternatively from the so-called displacement method, also postulated by Newman [8], which defines S_{op} as a level at which the last element in contact opens. The SY model can be activated in every load cycle, e.g. [9], or it may be triggered by the occurrence of some specified events, e.g. [3], the latter option involving reduced computer run times at the expense of computation accuracy. Obviously, aspects of the strip discretization, like the element sizing, rules for the element merging and splitting, etc., otherwise known to considerably affect the computed S_{op} levels, can be very distinct for various SY model implementations.

As it is well known, the original concept of Dugdale assumes plane stress conditions at the crack tip. In order to accommodate in the SY model a more general case of triaxial stress state, constraints on yielding the strip elements are imposed, as first proposed by Newman [3] and subsequently applied by others [4], [6], [7], [9], [10], [11], [12]. An equally important role of the associated constraint factors is, however, calibrating the model for a given material. In this way, various processes, which can influence crack growth but cannot be treated in a rigorous way, are covered indirectly. Because, as demonstrated elsewhere [12], SY model results are dramatically affected by the assumed constraints on local yielding, the selection of an appropriate constraint concept is of key importance.

A well known and most widely used SY model implementation is that included in the NASGRO software [13], currently commercially available. The user may choose between two different versions of the model, either one featuring a distinct constraint factor concept, and between several options of feeding the material data into the model. Reported by independent authors comparisons between observed crack growth and the NASGRO model predictions are confusing showing either a satisfactory, e.g. [14], or poor, e.g. [15], correlation between both type results. Typically, the authors confine themselves to applying only a single combination of the model type and the material data input option. Also, a limited scope of experimental results on crack growth considered in particular works does not enable to judge whether the model correctly predicts various empirical trends. For the above-mentioned reasons, the literature evidence is not very conclusive regarding the NASGRO SY model performance.

The goal of the present paper is to systematically evaluate the predictive capabilities of the NASGRO SY model. This is achieved through comparing the computed results obtained for a variety of analysis options available in the

NASGRO 3.0.21 software with the experimental data on crack growth generated for two different aluminium alloys under constant amplitude (CA) loading at several R-ratio values and under programmed and random VA load histories.

2. SY models in the NASGRO software

As said earlier, the NASGRO software contains two distinct implementations of the SY model termed in the NASGRO 3.0.21 manual [13] the constant constraint-loss (CCL) option and the variable constraint-loss (VCL) option. The CCL model developed by NASA and described in numerous publications by Newman (e.g. [3], [8], [16], [17]) employs a constraint factor on tensile yielding only, whilst constraint factors on compressive yielding are assumed to be unity both in the plastic zone and in the crack wake. The constraint factor value is the same for all elements in the tensile plastic zone and it is related to the fatigue crack growth rate (da/dN) according to Fig. 2, where $(da/dN)_1$ and $(da/dN)_2$ correspond to the beginning and end respectively of the transition from tensile mode crack growth to shear mode crack growth under CA loading. This concept stems from Newman's assumption that under CA loading the transformation of the fracture surface morphology is a manifestation of changing stress conditions at the crack tip from plane strain to plane stress, and hence of changing constraint [17]. Another premise for relating the constraint factor to da/dN have been experimental results indicating that for a given material under CA loading conditions the transformation is completed at approximately the same crack growth rate, irrespective of the R-ratio value [18]. In terms of the crack closure concept, such observations imply that the transition behaviour is controlled by the effective stress intensity factor range (ΔK_{eff}) defined as the difference between the maximum ($K_{\max}$) and the crack opening level (K_{op}) of the stress intensity factor in a fatigue cycle. With the CCL model, the constraint factor on tensile yielding varies linearly from its plane strain value (α_1) corresponding to fully tensile crack growth to the plane stress value (α_2) associated with fully shear crack growth, Fig. 2. The α_2 value is assumed to be 1.2 for all metals, whilst α_1 must be chosen by the user. The transition region spans 1.5 decades of da/dN and its central point $(da/dN)_{\text{trans}}$ is defined as a rate at which the cyclic plastic zone (computed from ΔK_{eff}) reaches a percentage of the specimen thickness.

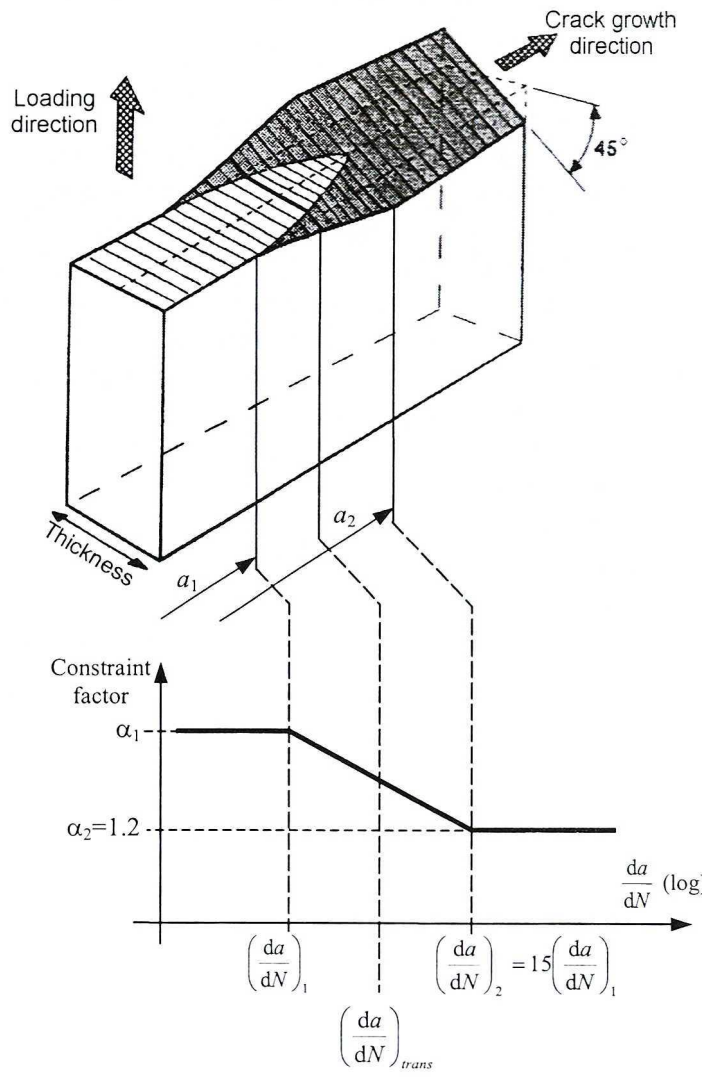

Fig. 2. Variations of the constraint factor on tensile yielding assumed in the CCL model

With the VCL model developed by National Aerospace Laboratory in the Netherlands [10], the constraint factor within the tensile plastic zone is assumed to decay from an α_{tip} value at the crack tip to a plane stress value of 1.15 at the plastic zone boundary, as shown in Fig. 3, where r_p is the tensile plastic zone size. The α_{tip} value is chosen by the program depending on the ratio of the plane stress plastic zone size to the specimen thickness (D/t). α_{tip} is set to its plane strain value of 2.35 for $D/t < 0.1$ and to its plane stress value of 1.15 if $D/t > 1.5$. Intermediate α_{tip} values are determined through

a piece-wise linear interpolation. Slightly different rules are used for the constraint factor distribution within the tensile primary and secondary plastic zone [1]. The values of constraint factors in the compressive plastic zone (α_c) and in the crack wake (α_w) are given by $\alpha_{tip}/\alpha_{new}$ and $1/\alpha_{new}$ respectively, where α_{new} is a material parameter declared by the user. As shown in Fig. 3, both constraint factors on compressive yielding are spatially constant. The available literature sources, e.g. [3], [10], suggest that the VCL model is numerically more complicated than the CCL model. The dependence of the constraint factor on the strip element position in the tensile plastic zone assumed in the VCL model requires iteration procedure to determine the primary plastic zone size. The influence function for an element due to the crack surface load acting on the same element is computed by numerical integration of the Westergaard solution because a distributed load over the element is assumed in that case. With the CCL model, all influence functions corresponding to the crack surface load can be solved analytically because a point force acting in the centre of an element is always assumed. Compared to the CCL model, the element sizes in the VCL model are smaller, which yields solving a larger number of compatibility equations at each load step.

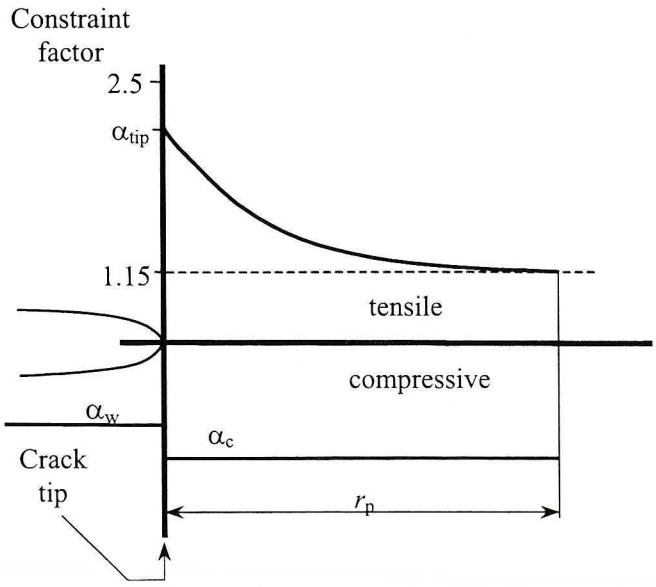

Fig. 3. Constraint factors in tension and compression assumed in the VCL model

[1] The tensile plastic zone developed in material that has not been plastically deformed before is termed primary. Otherwise it is termed secondary.

To run the SY model computations the material crack growth data must be defined in the input part of the program. The crack growth description can be available in the form of equations or in a discrete form as the the da/dN vs. ΔK_{eff} data. In either case, the material parameters may come from the user data base or from the NASGRO data base (NASMAT).

According to the NASGRO manual [13], the curve-fitting option utilizes the so-called NASGRO equation and the NLR equation, the latter employing the incremental crack growth concept [19]. However, only the NASGRO equation is considered below because with the NASGRO 3.0.21 software applied in the present study the NLR equation cannot be used for a new material, and because this equation parameters are not available for 2024 T3.

The NASGRO equation reads:

$$\frac{da}{dN} = C\left[\left(\frac{1-f}{1-R}\right)\Delta K\right]^n \frac{\left(1-\dfrac{\Delta K_{th}}{\Delta K}\right)^p}{\left(1-\dfrac{K_{\max}}{K_c}\right)^q} \tag{1}$$

where $f = \Delta K_{\text{eff}}/\Delta K$ represents the crack closure contribution, C, n, p and q are experimentally derived material parameters, ΔK_{th} is the threshold stress intensity factor range (a function of R) and K_{c} is the critical stress intensity factor.

For CA loading the f-function can be expressed according to Newman as [16]

$$f = \begin{cases} \max(R,\ A_0 + A_1 R + A_2 R^2 + A_3 R^3) & R \geq 0 \\ A_0 + A_1 R & -2 \leq R < 0 \end{cases} \tag{2a}$$

with the coefficients given by

$$A_0 = (0.825 - 0.34\alpha + 0.05\alpha^2) \cdot \left[\cos\left(\frac{\pi}{2} \cdot \frac{S_{\max}}{\sigma_0}\right)\right]^{\frac{1}{\alpha}} \tag{2b}$$

$$A_1 = (0.415 - 0.071\alpha) \cdot \frac{S_{\max}}{\sigma_0} \tag{2c}$$

$$A_2 = 1 - A_0 - A_1 - A_3 \tag{2d}$$

$$A_3 = 2A_0 + A_1 - 1 \tag{2e}$$

where the fitting parameters S_{max}/σ_0 and α should be chosen by the user.

For a material not included in the NASGRO data base, a *matgui* program available in the NASGRO software, which utilizes eqs (2a-e) can be used to curve fit to eq. (1) the user-declared da/dN vs. ΔK data obtained from tests under CA loading, preferably at several R-ratios. The user should also enter the aforementioned S_{max}/σ_0 and α parameters. The critical stress intensity factor K_c in Eq.(1) corresponding to the specific thickness can be declared by the user. Alternatively, the user may specify the fracture toughness value (K_{Ic}), thus enabling the *matgui* program to determine K_c from an empirical equation produced in the Manual [13]. ΔK_{th} in Eq.(1) is determined by *matgui* as a function of R and material parameters ΔK_o, C_{th}^+ and C_{th}^- using an empirical relationship given in [13]. ΔK_o, C_{th}^+ and C_{th}^- can be directly entered by the user or automatically chosen by the program from user declared data on the threshold stress intensity range at several R-ratios. It is assumed that if $R > R_{cl}$, where R_{cl} is the so-called cutoff stress ratio defined by the user, the ΔK_{th} value is constant, i.e. independent of R. The p and q exponents, which control the "knees" of the crack propagation curve in the lower and upper region respectively must be chosen by trial and error to fit the corresponding da/dN vs. ΔK data. The C and n constants can be chosen either in the same way or automatically by the *matgui* program.

The α parameter represents the α_1 value for the CCL model and the α_{new} value when the VCL model is used. Thus, α serves to scale the constraint factors values for either model and, as such, it has a profound effect on the computation results. It is suggested in the NASGRO manual [13] that irrespective of how the material crack growth data are described, i.e. using the NASGRO equation or in a discrete form, a number of SY model predictions on crack growth should be run for CA loading in order to fix the α value which produces the best fit to the observed results. This implies that if the NASGRO equation is used, the curve-fitting procedure according to the *matgui* program enables to choose a preliminary α value only. To apply the SY model, the monotonic material properties (yield stress S_y and ultimate strength S_u) must be specified in addition to the material data entered earlier.

When the NASGRO equation is used, the constraint factor incorporated in the CCL model is assigned a constant value of α_1. Executing the CCL model with the constraint factor varying according to Fig. 2 is only possible when the crack growth rates are described in a discrete form as the da/dN vs. ΔK_{eff} data (the so-called 1-D table).

In NASGRO, a load time history is in the form of discrete sequence of the load minima and maxima and can be entered from keyboard or from a file. It is defined as a schedule of blocks, where each block may contain a number of steps. A load step consists of one or more CA cycles. The SY model can be run in two computation speed modes. The "fast" mode is suitable when it is known that the crack opening stress will stabilize at some point in the load history. The model is used only until that stable S_{op} level is attained. With the "full" mode, the model is used to compute S_{op} throughout the entire load history. However, because the SY model solution is very time consuming, even in the case of the "full" mode provisions are made in the software to avoid triggering the S_{op} calculations cycle-by-cycle. S_{op} is always determined for the first cycle of any load step and it is computed at least five times if the step contains more than 5 cycles. For CA loading, it implies that increasing the number of cycles in a load step yields less frequent S_{op} calculations and, hence, a declined accuracy of the predictions. For VA spectra it is possible to consider only most significant cycles for the SY model solution. The difference in the applied stress ΔS_{max} from one "significant" maximum (minimum) load to the next required to trigger the S_{op} calculations and the maximum number of cycles ΔN_{max} that can be spent in a crack growth increment between the calculations are declared by the user.

3. Experimental program

The sheet materials used are two aluminium alloys, namely the Russian alloy D16CzATWH with a nominal thickness of 4 mm delivered in the clad condition, the thickness of the cladding layers being approximately of 0.1 mm, and the 2 mm thick bare 2024-T3 material. The measured mechanical properties of both metals are $S_y = 335$ and 394 MPa, $S_u = 457$ and 502 MPa, elongation 22 and 19% for D16 and 2024-T3 respectively. As specified elsewhere [20], the chemical composition of both materials are alike except that the Russian alloy shows a lower content of Fe and Si, thus appearing a higher purity metal. Consequently, the crack growth behaviour of D16 is in good agreement with that noted for 2024-T3 under similar loading conditions [20].

The fatigue crack growth tests were carried out on middle cracked tension specimens with a central starter notch provided as a narrow saw cut. The specimen width was 100 mm for both D16 and 2024-T3. The loading conditions for all tests are specified in Table 1. The VA Type I–III tests with periodic overloads and underloads are considered to be simplified service-simulating tests representing stresses on the wing structure due to bending.

Table 1.

Loading conditions in the crack growth tests (stress levels in MPa)

Material	Type of loading		Baseline cycles				m	S_{OL}	S_{UL}	S_{max} (miniFALSTAFF)
			S_{min}	S_{max}	ΔS	R				
D16CzATWH	CA		-26.7	53.3	80	- 0.5	-	-	-	-
			0	64	64	0				
			0	140	140					
			32	96	64	0.33				
			35	140	105	0.75				
	Single OL		0	64	64	0	-	128	-	-
	VA	Type I	32	96	64	0.33	10	-	0	-
		Type II						128	-	-
		Type III						128	0	-
		mini FALSTAFF	-	-	-	-	-	-	-	247.5
			-	-	-	-	-	-	-	230
			-	-	-	-	-	-	-	220
2024-T3	CA		40	120	80	0.33	-	-	-	-
			0		120	0	-	-	-	-
			- 40		160	- 0.33	-	-	-	-
			- 80		200	- 0.67	-	-	-	-
			40	160	120	0.25	-	-	-	-
			0		160	0	-	-	-	-
			- 40		200	- 0.25	-	-	-	-
			- 80		240	- 0.5	-	-	-	-
			40	200	160	0.2	-	-	-	-
			0		200	0	-	-	-	-
			- 40		240	- 0.2	-	-	-	-
			- 80		280	- 0.4	-	-	-	-
	VA	Type I	40	120	80	0.33	5	-	0	-
								-	-80	-
							100	-	0	-
								-	-80	-
		Type II	40	120	80	0.33	5	160	0	-
								160	-80	-
								200	0	-
								200	-80	-
							100	160	0	-
								160	-80	-
								200	0	-
								200	-80	-

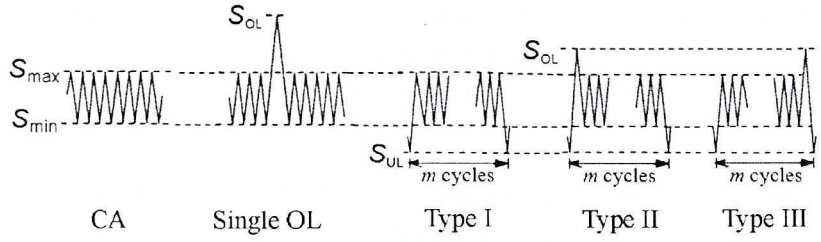

Here, the larger cycle should simulate the so-called air-ground-air transition, whilst the smaller CA cycles should represent the loads due to air turbulence. For the D16 material, tests under a more realistic service-simulating loading,

namely the miniFALSTAFF sequence, were also executed. As specified in Table 1, three levels of the maximum stress (S_{max}), which characterizes the spectrum severity, have been considered in the latter experiments. The fatigue crack growth responses observed in the tests listed in Table 1 are presented and discussed in detail in refs [20] and [21] for D16 and 2024-T3, respectively. These works revealed that retarded crack growth always occurred for the load histories of Type II and III and for miniFALSTAFF, as indicated by the conservative non-interaction, i.e. based on the CA test data, predictions on crack growth rates. The most significant load interaction effects were exhibited under the miniFALSTAFF history, for which the predicted rates exceeded about three times the measured values. Perhaps a most surprising observation for D16 was that the crack growth life under the Type III sequence was about 27% longer than under the Type II sequence. Consistent with the plasticity-induced crack closure based interpretation, the reported literature data indicate that a single underload-overload excursion typically yields a larger retardation effect during the subsequent smaller amplitude cycles than an overload-underload sequence [22]. The present results demonstrate that, if the larger cycles are applied periodically, an opposite behaviour may occur for a certain combination of the loading parameters and material. The experimental trends revealed in the VA tests on 2024-T3 are discussed in more detail in section 5. Altogether, the present VA test results imply a complex nature of the load interaction phenomena which is a challenge for crack growth prediction models.

4. Prediction results for the D16 alloy

Only the user experimental results are the source of the material data for D16, because this material is not included in the NASMAT data base. The predictions have been made for the CCL model and the VCL model, in either case considering the material data input through the NASGRO equation and in the form of the discrete da/dN vs. ΔK_{eff} data.

All computations have been run in the "full" mode. With the CA loading, the simulation results indicate an insignificant effect of the number of cycles set for one load step. For example, in the case of the $R = 0.33$ test, a 3 per cent difference was found in the fatigue lives estimated for 10 and 1000 cycles per load step. For the programmed VA loading, 10 cycles per step have been set in all analyses. With the miniFALSTAFF sequence, ΔS_{max} = 3 MPa and $\Delta N_{max} = 20$ cycles have been taken, which for this type load history actually implies the cycle-by-cycle S_{op} computations.

4.1. Curve fitting the crack growth data using the NASGRO equation

Because the crack growth data within the near-threshold region have not been generated in the fatigue tests, the required material constants $\Delta K_o = 3.2$ MPa$\sqrt{\text{m}}$, $C_{th}^{+} = 1.5$, $C_{th}^{-} = 0.1$, $R_{cl} = 0.7$ and $p = 0.5$ have been set, as specified in the NASGRO manual for Al 2024-T3 clad material. Based on the present fatigue tests on D16, K_c =51 MPa$\sqrt{\text{m}}$ has been let for the considered thickness of 4 mm. The values of the other material constants, namely $C = 0.58 \cdot 10^{-10}$ (da/dN in mm/cycle, ΔK in MPa$\sqrt{\text{mm}}$), n = 2.57, $S_{max}/\sigma_0 = 0.3$ and $q = 0.4$ have been chosen by guesses to get and adequate curve fitting for the experimental crack growth data. It has been noted that an automatic selection of the C and n constants using the *matgui* program does not enable a satisfactory approximation of the test data by the curves.

Though in NASGRO aluminium alloys are assigned the α value of 1.9 or 2.0 [13], [23], a satisfactory curve fit of the experimental data could not be obtained for the α parameter below 2.2. However, even with such a high α value, both the CCL model and VCL model have been found to exaggerate the effect of R under CA loading. It has been further noted that correlating the R-ratio effect for all tests performed is never achieved if still higher α values are used. Eventually, the α value of 2.85, which for both models provides correct simulation results for the $R = 0.33$ test has been fixed in the analyses performed for VA loading, simply because the baseline cycles in the Type I – III tests (compare Table 1) have been applied at this stress ratio. Increasing the α value from 2.2 to 2.85 did not affect noticeably the correlation between the experimental da/dN vs. ΔK data and the corresponding curve fit derived from the *matgui* program. Fig. 4 shows the crack growth test results plotted together with the approximating curves. Presented in Fig. 5a and b are the ratios of predicted to observed fatigue crack growth life (N_{NASGRO}/N_{EXP}) for the CCL model and VCL model, respectively. Compared to the CCL model, the VCL model correlates slightly better the test results. As seen in this figure, for both models more safe, i.e. closer to unity life ratios are obtained with $\alpha = 2.85$ than for $\alpha = 2.2$. It must be emphasised, however, that neither of the above α values enables reproducing the retardation behaviour following a single overload, as exemplified in Fig. 6 by the CCL model results.

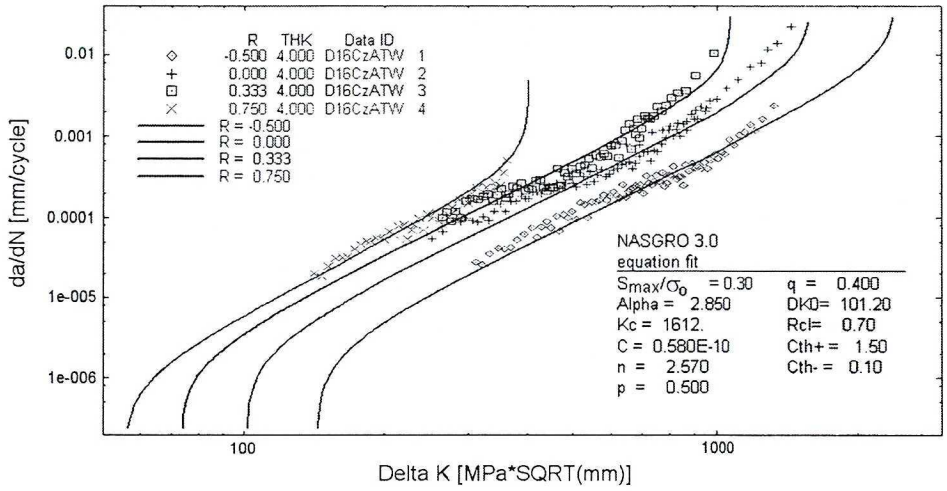

Fig. 4. The CA test results for D16 and their curve fit to eq. (1)

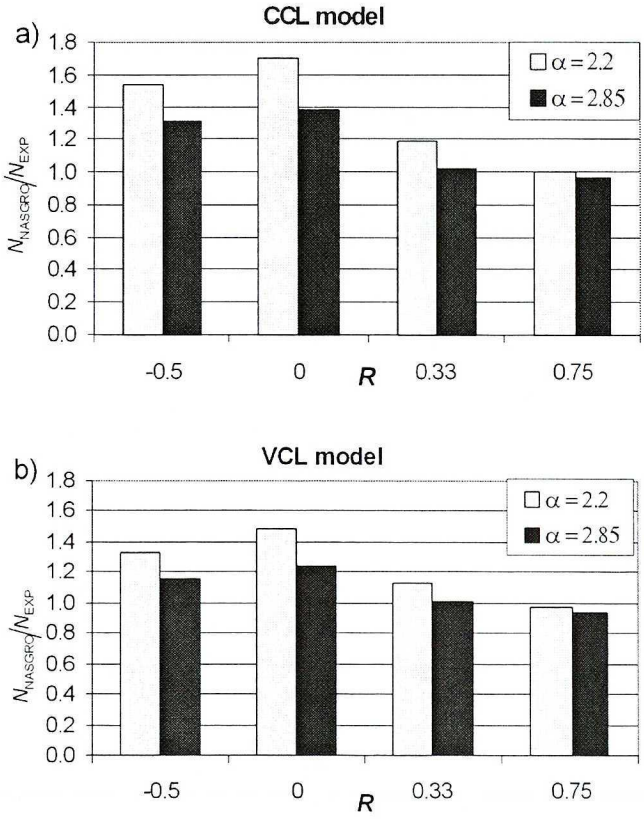

Fig. 5. Predicted-to-observed crack growth life ratios for the CA tests on D16: (a) CCL model; (b) VCL model. The predictions are based on the NASGRO crack growth equation

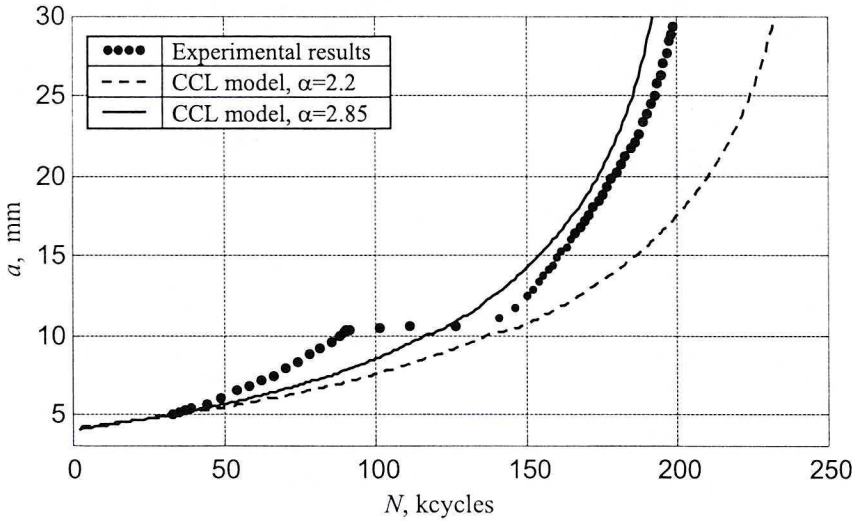

Fig. 6. Comparisons between crack growth curves observed for the OL test on D16 and predicted by the CCL model for two α-values. The predictions are based on the NASGRO crack growth equation

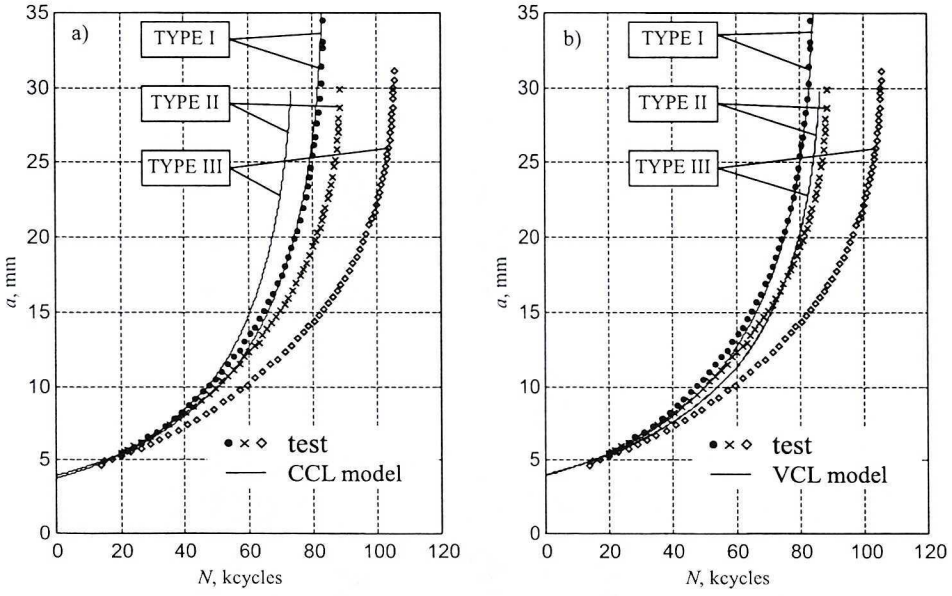

Fig. 7. Comparisons between the observed and predicted crack growth curves for the simplified service-simulating tests on D16: (a) CCL model; (b) VCL model. The predictions are based on the NASGRO crack growth equation

In Fig. 7, observed and predicted crack growth curves for the simplified service-simulating tests are compared. It is seen that both models correctly reproduce the effect of underloads for the Type I sequence. The CCL model

erroneously predicts that the load histories of Type II and Type III are more detrimental than Type I. Unlike the CCL model, the VCL model yields correct results also for Type II loading. Neither model accounts, however, for the beneficial effect of the Type III load sequence compared to Type II. Though some experimental trends are not correctly mirrored by the predictions, the quantitative agreement between the computed and observed total crack growth lives appears, according to commonly applied criteria for the evaluation of predicted results, still satisfactory as the N_{NASGRO}/N_{EXP} ratios range from 0.67 to 1.0. Again, the VCL model results are more accurate than those from the CCL model.

The life ratios for the miniFALSTAFF sequence are produced in Fig. 8. The same value of the N_{NASGRO}/N_{EXP} ratio for all S_{max} levels would indicate a correctly reflected S_{max} impact on the fatigue life. In this respect, the VCL model performance is slightly better and its predictions exhibit a smaller amount of conservatism compared to those from the CCL model.

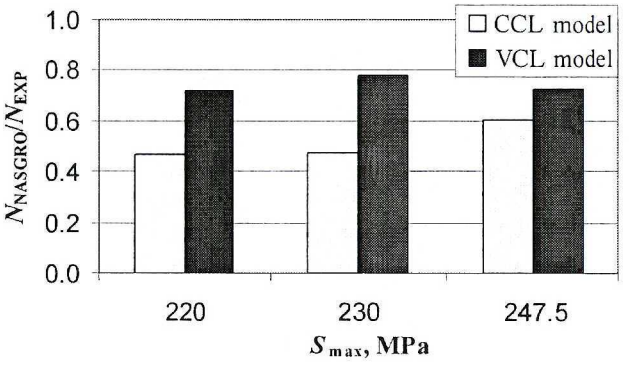

Fig. 8. Predicted-to-observed crack growth life ratios for D16 under the miniFALSTAFF load sequence. The predictions are based on the NASGRO crack growth equation

4.2. The crack growth data in the discrete form (1-D table)

In order to create the input material data in the discrete form, the da/dN vs. ΔK results from all CA tests have been converted into the da/dN vs. ΔK_{eff} data. With this purpose, an equation by Schijve [24]

$$U = \frac{\Delta K_{eff}}{\Delta K} = 0.55 + 0.33R + 0.12R^2 \tag{3}$$

has been applied first. The resulting da/dN vs. ΔK_{eff} data are plotted in Fig. 9 together with the corresponding trend line obtained using the cubic

smoothing spline technique. In Fig. 9, the data-points in the low crack growth rate region which, as mentioned before, are lacking from the test on D16, have been imported from the 1-D table for Al 2024-T3 available in the NASMAT data base. Thus, the 1-D table used in the analyses below combines the discrete data from the aforementioned trend line for D16 (open stars in Fig. 9) and from the NASMAT data for 2024-T3 (closed stars in Fig. 9).

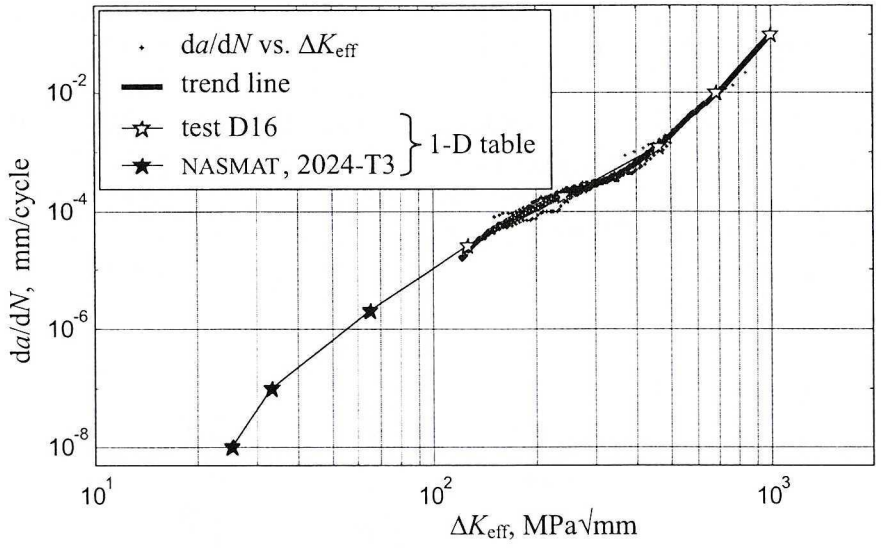

Fig. 9. The discrete d*a*/d*N* vs. ΔK_{eff} data points (1-D table) for D16 based on the *U* value according to eq. (3) (see text)

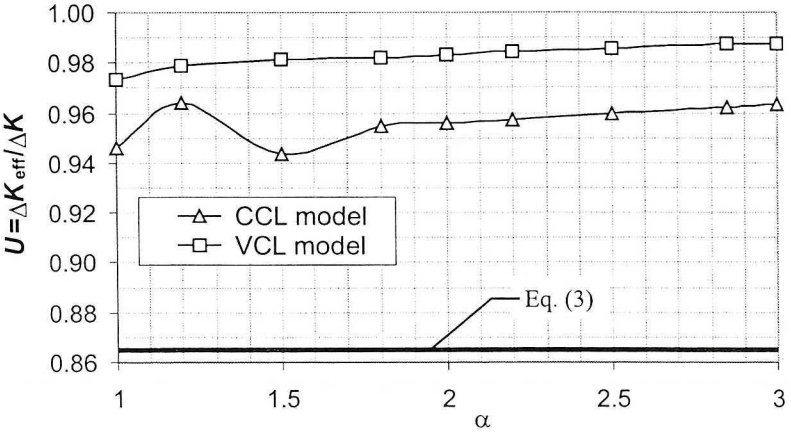

Fig. 10. Average *U*-values computed by the NASGRO SY models for D16 at $R = 0.75$ for a range of α values

For $R = 0.75$ eq. (3) yields U of 0.865. However, neither the CCL model nor the VCL model are capable of predicting such a high amount of crack closure at this stress ratio even for $\alpha = 1$, as illustrated in Fig. 10. It is, therefore, not surprising that if the da/dN vs. ΔK_{eff} data based on eq. (3) are employed, a very poor correlation of the R-ratio effect under CA loading is noted for either model irrespective of the α value.

It has been further found that the U-estimates according to eq. (2) agree with those from eq. (3) for S_{max}/σ_0 of 0.37 and $\alpha = 1$. For $S_{max}/\sigma_0 = 0.3$ suggested in the Manual [13] and higher values of α eq. (2) always yields the U estimates exceeding those from eq. (3), as exemplified in Fig. 11 for $\alpha = 2.0$. Also plotted in this figure are average results on U computed for all CA tests using the SY models incorporating the latter α value. It is seen that both models yield U estimates very close to those according to eq. (2).

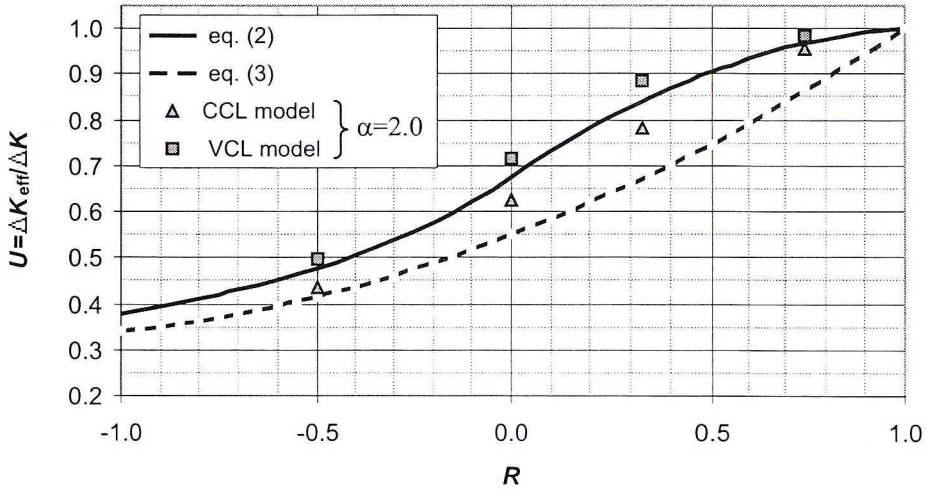

Fig. 11. U vs. R plots according to eqs. (2) and (3) with $S_{max}/\sigma_0 = 0.3$ and $\alpha = 2.0$ and SY models results (see text)

Viewing the results shown in Figs 10 and 11, the next approach was to incorporate in the 1-D table the test results for D16 processed using eq. (2) with $\alpha = 2.0$ and $S_{max}/\sigma_0 = 0.3$ rather than using eq. (3), the NASMAT data for 2024-T3 within the low da/dN regime remaining the same as in Fig. 9. Through entering guesses for the α values and running the SY model computations for the CA tests, a best overall fit to the experimental data has been achieved with $\alpha = 2.85$ for the CCL model and $\alpha = 2.0$ for the VCL model. The corresponding N_{NASGRO}/N_{EXP} ratios are provided in Fig. 12. For both models, the correlation of the R-ratio effect is better than in Fig. 5. Compared to the CCL model, the VCL model incorporates a more realistic

α value and it yields slightly more accurate results evidenced by the N_{NASGRO}/N_{EXP} ratios close to unity. For that reason, only the VCL model is further applied in the analyses for VA loading.

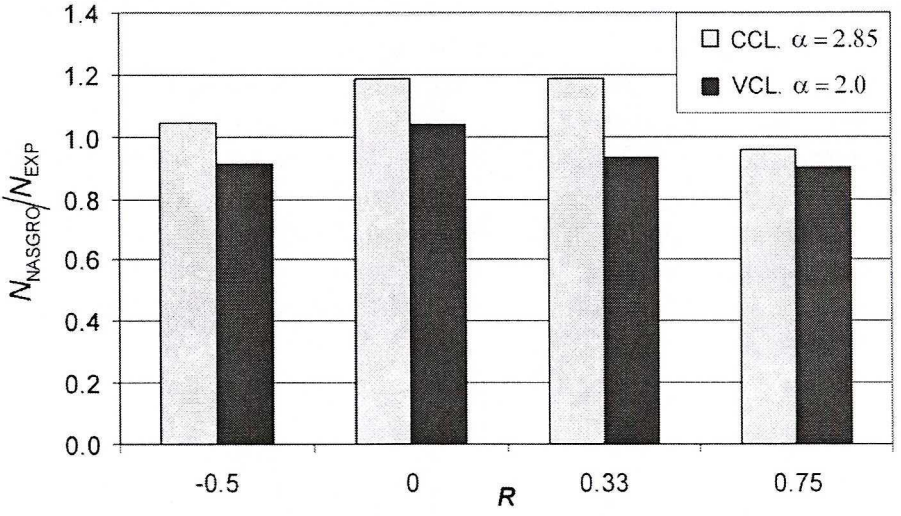

Fig. 12. Predicted-to-observed crack growth life ratios for the CA tests on D16. The predictions are based on the 1-D table & eq. (2)

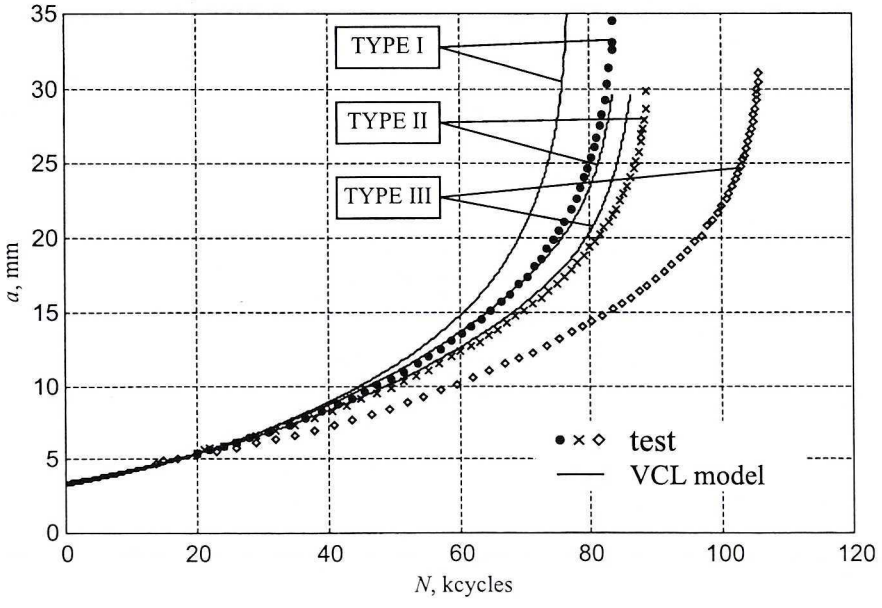

Fig. 13. Comparison between the observed and predicted using the VCL model crack growth curves for the simplified service-simulating tests on D16. The predictions are based on the 1-D table & eq. (2)

The computation for the single overload test indicates that for neither model the overload application is mirrored by the predicted α vs. N curve, which remains smooth at this point. It is seen in Fig. 13, where the computed and observed α vs. N curves for the simplified flight simulation tests are produced that, compared to the results shown in Fig. 7b, the VCL model does account for the different amounts of the load interaction effects under the sequences of Type II and Type III, but the predictions for Type III loading still remain more conservative than those for Type II. Surprisingly enough, the predictions for miniFALSTAFF resulting from the discrete input data and shown in Fig. 14 are much worse than those based on the NASGRO equation (compare Fig. 8). The latter results imply that an analysis option which enables a superior reproducing by the model the R-ratio effect in CA tests does not necessarily lead to an improved prediction quality for VA loading.

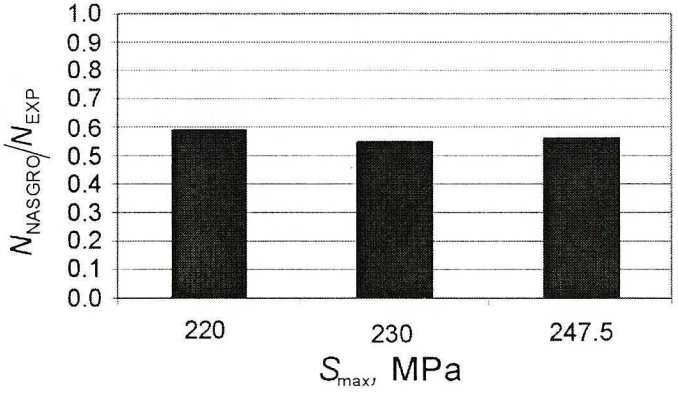

Fig. 14. Ratios of the predicted using the VCL model to observed crack growth lives for D16 under the miniFALSTAFF load sequence. The predictions are based on the 1-D table & eq. (2)

5. Prediction results for the 2024-T3 alloy

With 2024-T3, the primary intention of the authors has been to evaluate the NASGRO SY model performance when the material data are imported from the NASGRO data base (NASMAT). Because the NASGRO 3.0.21 data base contains the NASGRO equation parameters for 2024-T3 clad material only, the parameters for the bare material available in the demo version of NASGRO 4.02 have been entered manually. In all computations $\alpha = 2.0$ and $S_{max}/\sigma_0 = 0.3$ assigned to 2024-T3 in NASMAT have been used. For the CA loading case, all four combinations of the model and the material data input type, namely CCL model & eq. (1), CCL model & 1-D table, VCL model & eq.(1) and VCL model & 1-D table have been considered. The corresponding predicted-to-observed life ratios are depicted in Fig. 15. It is

seen that no analysis option enables a satisfactory correlation of the R-ratio influence. All predictions are conservative, these from the VCL model being more so than from the CCL model. For the $R = 0$ tests, the predictions from all four options become more conservative with increasing the S_{max} level. Altogether, the best, i.e. the least conservative predictions are derived for the CCL model & 1-D table combination whilst the VCL model & 1-D table yields the worst, that is the most conservative results.

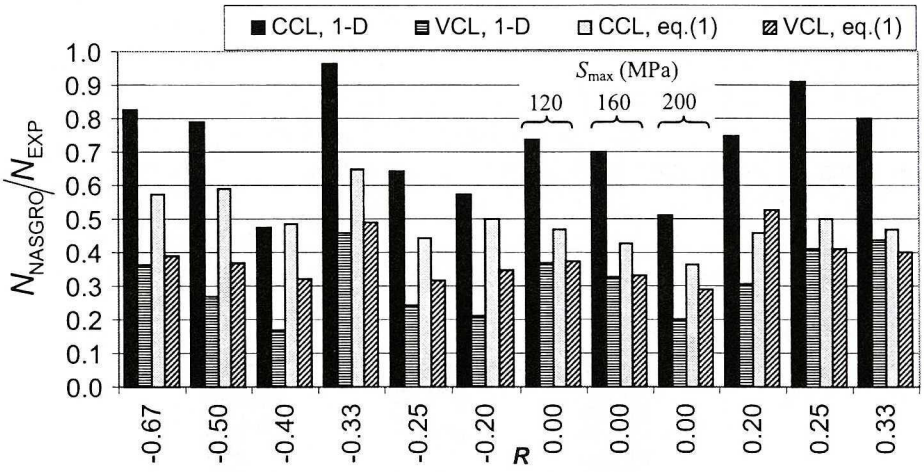

Fig. 15. Predicted-to-observed crack growth life ratios for the CA tests on 2024-T3 for various combinations of the model and material data input type

The reason for the very poor prediction results for the CA tests can be understood by comparing the actual material data observed in the fatigue tests with those according to the NASGRO data base. Fig. 16 depicts the experimental da/dN vs. ΔK results for several R-ratios and the corresponding curves according to eq. (1) incorporating the material constants from the NASMAT files. The latter have been plotted using the *matgui* program. It is clear from Fig. 16 that the overly conservative predictions derived from either model if coupled with eq. (1) stem from systematic overestimating by the NASGRO equation the crack growth rates in the Paris regime. Similarly, Fig. 17 shows that all NASMAT 1-D table data-points 2024-T3 fall above the da/dN vs. ΔK_{eff} test data. The latter have been derived through processing the observed da/dN vs. ΔK data using eq. (2) with the same values of α and S_{max}/σ_0 as for the predictions presented in Fig. 15. Recalling from Fig. 11 that closure levels predicted by both SY models for α =2.0 fall close to those computed from eq. (2) incorporating the same α value, it is obvious from Fig. 17 that conservative predictions must result if the model is fed with the

crack growth law according to the NASMAT 1-D table data. It noteworthy in Fig. 11 that the CCL model estimates on U fall below the values computed from eq. (2), whilst the U values according to the VCL model are higher than the levels given by eq. (2). Fig. 15 demonstrates that in line with the above, the 1-D table based predictions from the VCL model show by far more conservatism than the CCL model results.

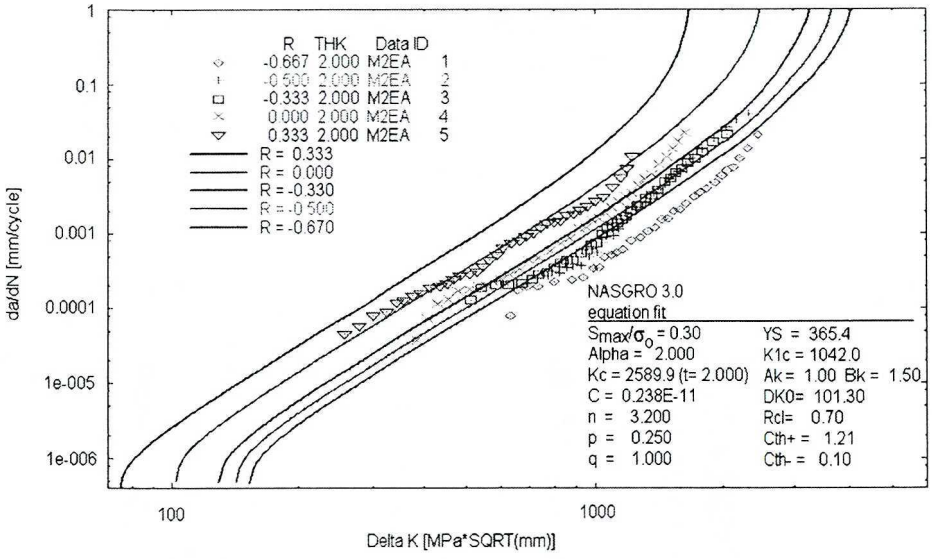

Fig. 16. Curve fit to eq. (1) according to NASMAT data base at several R-ratios for 2024-T3 and the corresponding CA test results

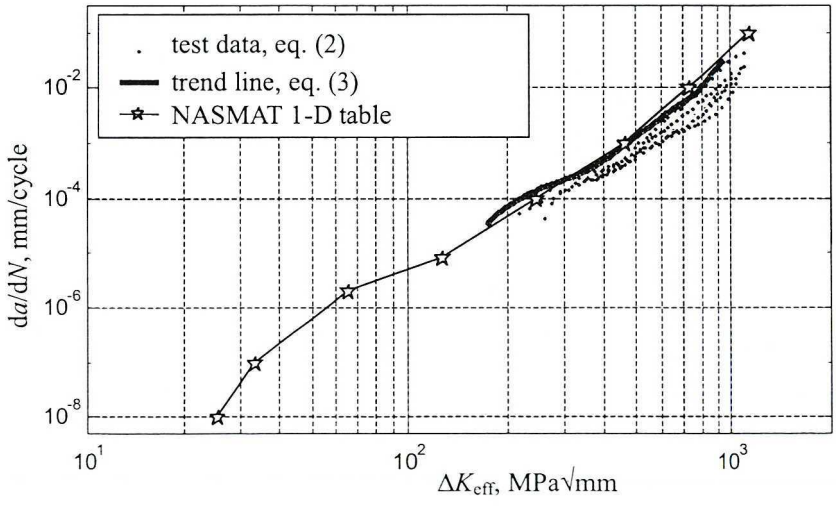

Fig. 17. The NASMAT 1-D table data points for 2024-T3, the experimental crack growth data processed using eq. (2) and the experimental trend line corresponding to eq. (3) (see text)

Eq. (3) has been found to enable a superior to eq. (2) consolidation of the da/dN vs. ΔK_{eff} results for 2024-T3. Fig. 17 indicates that the trend line obtained using the spline technique for the da/dN vs. ΔK_{eff} data corresponding to eq. (3) turns out to match quite well the NASMAT 1-D table data. As said in section 4.2, the U-estimates from eq. (2) tend to those according to eq. (3) when α is decreased. Viewing the above and considering that for a given value of the α-parameter the NASGRO SY model results on closure levels are close to those given by eq. (2), compare Fig. 11, the next analysis step has been to evaluate the performance of the CCL model coupled with the 1-D table (the "best" computation option from Fig. 15) for $\alpha = 1.2$, at the same time the lowest possible constraint factor value. From Fig. 2 it is clear that in that case the constraint factor will remain constant throughout the simulations.

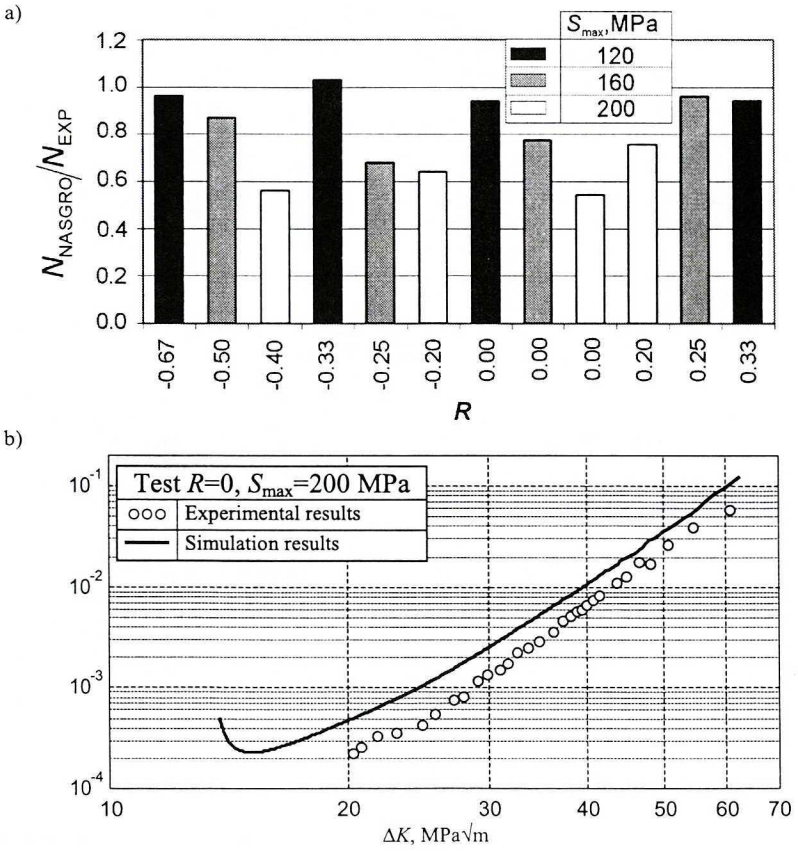

Fig. 18. Comparisons between the experimental results and the predictions from the CCL model & 1-D table option, $\alpha = 1.2$, for the CA tests on 2024-T3: (a) the predicted-to-observed life ratios; (b) the predicted and observed crack growth rates for $R = 0$, $S_{max} = 200$ MPa test

Fig. 18a gives the computed-to-observed life ratios resulting from the CCL model & 1-D table option with α of 1.2 for the CA tests. As expected, all N_{NASGRO}/N_{EXP} values are now higher, i.e. closer to the unity than for $\alpha = 2$ (compare Fig. 15). It is seen that, regardless of the stress ratio, the worst results correspond to the highest S_{max} stress value of 200 MPa whilst the best predictions are obtained for S_{max} = 120 MPa. The reason why for the S_{max} = 200 MPa tests the largest discrepancies between the observed and computed data have always occurred in the initial part of each experiment, as exemplified in Fig. 18b, remains unclear because the LEFM conditions are satisfied throughout the prevailing part of the tests.

The predictions for the VA loading tests on 2024-T3 mainly served the purpose of recognizing whether the model could correctly describe the observed experimental trends due to the change of the test variables. As evident in Table 1, for both type VA load histories the variable test parameters were the underload level S_{UL} and the number of cycles in the loading block m. In addition, for Type II loading the effect of the overload level S_{OL} was studied.

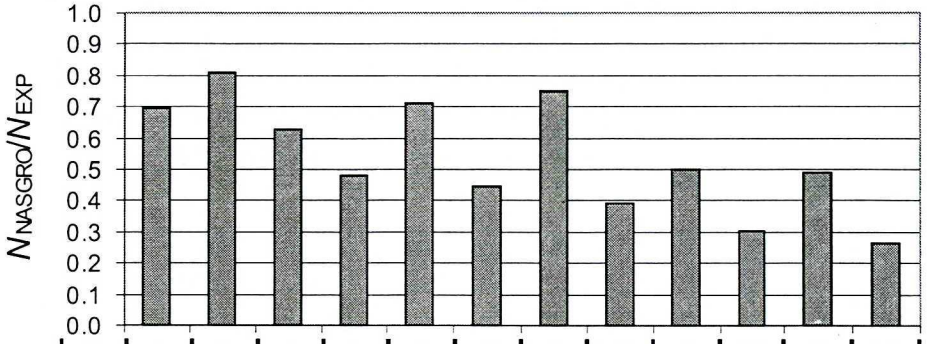

No.	1	2	3	4	5	6	7	8	9	10	11	12
m	5	100	5	100	5	100	5	100	5	100	5	100
S_{OL}	-	-	-	-	160	160	200	200	160	160	200	200
S_{UL}	0	0	-80	-80	0	0	0	0	-80	-80	-80	-80
	Type I				Type II							

Fig. 19. Ratios of the predicted using the CCL model to observed crack growth lives for all VA tests on 2024-T3 (stress levels in MPa). The predictions are based on the 1-D table, $\alpha = 1.2$

Fig. 19 shows the simulation results for all VA tests in terms of the ratios of the predicted-to-observed total crack growth life, whilst the absolute predicted and observed lives are provided in Fig. 20. As seen in Fig. 20, the model predicts against the experimental results that for the longer loading block (m = 100) the more compressive underload $S_{UL} = -80$ MPa, Test 4, yields a shorter crack growth fatigue life compared to that for $S_{UL} = 0$, Test 2.

It is noteworthy that the latter experimental trend remains in disagreement with the concepts of plasticity-induced crack closure and residual stresses ahead of the crack tip, since both mechanisms imply that a more severe underload should induce more detrimental load interaction effects, i.e. faster crack growth during the subsequent smaller amplitude cycles than a less severe underload [22]. Because with the SY model the load interaction phenomena are attributed to plasticity-induced crack closure and the computed crack opening stress is influenced by the residual stresses, the erroneous prediction on the S_{UL} effect in Tests 2 and 4 is not surprising.

The detailed analysis of the predictions, Fig. 20, reveals that except the latter case, all other experimental trends, which otherwise can be rationalized in terms of crack closure, are correctly mirrored by the computed results. Regarding the effect of the S_{UL} level, the model adequately predicts that crack growth under a load sequence with $S_{UL} = -80$ MPa is always faster than under S_{UL} of zero if all other loading parameters remain unchanged. Thus, the fatigue life for Test 1 is shorter than for Test 3, Fig. 20. Similarly, the computed fatigue lives for Tests 9, 10, 11 and 12 exceed those for Tests 5, 6, 7 and 8, respectively, in accordance with the observations.

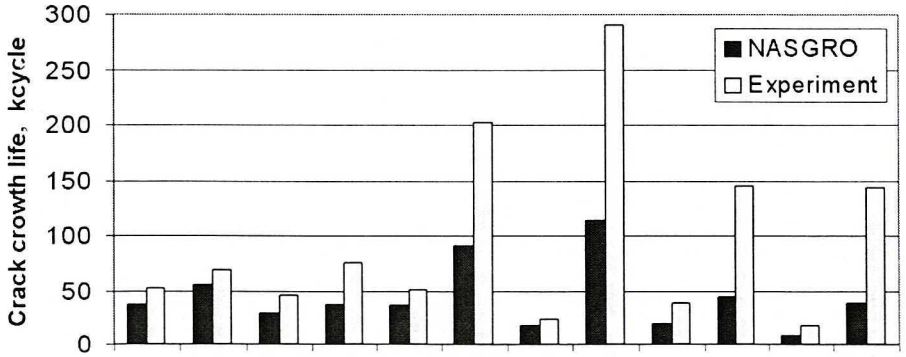

No.	1	2	3	4	5	6	7	8	9	10	11	12
m	5	100	5	100	5	100	5	100	5	100	5	100
S_{OL}	-	-	-	-	160	160	200	200	160	160	200	200
S_{UL}	0	0	-80	-80	0	0	0	0	-80	-80	-80	-80
	Type I				Type II							

Fig. 20. Comparisons between the crack growth lives observed in all VA tests on 2024-T3 and the predictions from the CCL model & 1-D table option, $\alpha = 1.2$ (stress levels in MPa)

Fig. 20 further reveals that the model adequately predicts the character of the load interaction effects for the sequences of Type II containing the overload cycles compared to the respective Type I sequences. For load

histories with overloads applied periodically among smaller amplitude baseline cycles, reapplication of an overload reactivates mechanisms which lead to crack growth retardation, but at the same time the overload may interrupt the retardation process due to the preceding overload. Also, a major part of the crack advance occurs during the overload cycles [22]. As seen in Fig. 20, in the case of Type II loading with $m = 5$, the detrimental load interaction effects overweigh the beneficial ones, because the overload spacing is insufficient to enable development of crack growth retardation during the baseline cycles. In agreement with the experimental observations the computed lives for Type I No. 1 and 3 load histories are slightly longer than under Type II No. 5 and 9 loading respectively, Fig. 20. Similarly, the results in Fig. 20 indicate that the model correctly predicts that Type II No. 7 and 11 sequences yield faster crack growth than Type I No. 1 and 3 sequences, respectively. The experimental observations revealed that for the load blocks with $m = 100$ the beneficial effects of the overload cycles prevailed, as evidenced in Fig. 20 by the crack growth lives significantly longer in Type II No. 6 and No. 8 tests compared to Type I No. 2 test and by the lives under Type II No. 10 and No. 12 load sequence exceeding the life for Type I No. 4 loading. All these trends are reproduced by the simulated results.

For Type II loading, the predicted trends associated with the effect of the S_{OL} level are again in accordance with the experimental observations. Thus, for $m = 5$ the larger overloads ($S_{OL} = 200$ MPa) appear more detrimental than the smaller overloads ($S_{OL} = 160$ MPa), as indicated in Fig. 20 by the shorter predicted life for Test 7 compared to Test 5 and for Test 11 compared to Test 9. From Fig. 20, the reversed trend revealed in the experiments with the less frequently applied overloads ($m = 100$) and $S_{UL} = 0$ is also followed by the predictions. Specifically, the predicted life for Test 8 is longer than for Test 6 whilst in the case of $S_{UL} = -80$ MPa, Test 10 and 12, the predicted lives are almost the same, again in agreement with the observed results.

It should not be overlooked that also the effect of the loading block length m is described in the qualitative agreement with the tests results, which implies that the predicted life for a short block ($m = 5$) is always considerably shorter than the life for a long block ($m = 100$) if the stress levels are the same for both blocks, Fig. 20.

For more than one reason, the quantitative correlation between the predictions and the test results specified by the life ratios in Fig. 19 cannot be considered satisfactory. In several cases the N_{NASGRO}/N_{EXP} values drop below 0.5 which, according to commonly accepted criteria, implies overly conservative predictions. Further, the data produced in Fig. 19 indicate that the model always yields less accurate, i.e. more conservative, results for a loading

block of $m = 100$ compared to its shorter counterpart ($m = 5$), the predictions for No. 1 and No. 2 tests being the only exception. Obviously, the worse model performance for the longer blocks can be attributed to an inadequate allowance for the load interaction effects which have been considerably more significant in the case of the longer spacing between the larger cycles. Specifically, the most inadequate predictions ($N_{NASGRO}/N_{EXP} < 0.5$) correspond to No. 6, 8, 10, 12 tests with the rarely applied overloads. At the same time, systematic underestimating by the model the beneficial influence of the overloads in the $m = 100$ load histories becomes also evident from comparisons of the life ratios for Type I tests with the values for appropriate Type II tests. Thus, the values of the life ratio corresponding to Type II Test 6 and Test 8 are twice lower than for Type I Test 2. Similarly, the ratios for Type II No. 10 and 12 tests are half the value corresponding to Type I No. 4 test.

6. Discussion

While evaluating the NASGRO SY model prediction capabilities, it cannot be overlooked that altogether significantly better results both for the load histories of Type I and II from the Misawa and Schijve experiments [21] and for the miniFALSTAFF sequence have been obtained by Padmadinata using the CORPUS model for crack growth predictions [25]. Specifically, the predicted-to-test crack growth life ratios for Type I and II loading reported in the latter study range from 0.81 to 1.27, and in the case of miniFALSTAFF they amount to 0.88 and 0.9 for two different characteristic stress levels. The CORPUS model belongs to the category of crack closure-based semi-empirical prediction concepts, which compared to the SY model are by far less sophisticated and, hence, involve much shorter computation time.

Perhaps the most important finding of the present study is that no computation option enabled to describe retarded crack growth after a single overload cycle in the test on D16. Consequently, the NASGRO SY model produced overly conservative results for load sequences with periodically applied overloads, namely Type II and Type III histories. As seen in Figs. 19 and 20, the amount of conservatism (evidenced by the predicted-to-test crack growth life ratios falling even below 0.3) increased with the overload level (S_{OL}) and the overload spacing (m), thus indicating that the model systematically underestimated the beneficial effects of the overloads. The above observations definitely question the utility of the NASGRO model for spectra steep in the low frequency range, when retardation can take long periods of smaller amplitude cycles between rarely occurring high loads.

The model calibration for a new material is far from being straightforward. A satisfactory curve fitting the CA crack growth data using the NASGRO equation can be obtained for a range of the α-parameter values (e.g. from 2.2 to 2.85 for D16) and, hence, it does not guarantee satisfactory prediction results from the SY models. For either of the two NASGRO SY models, the "best" value of the α-parameter must be chosen by guesses to achieve most satisfactory crack growth predictions for CA loading at various R-ratio values. A highly disadvantageous feature of the model behaviour revealed in the present analyses is that improving the predictions for CA loading, which in general are unconservative and tend to exaggerate the R-ratio effect, would require using still higher values of the fitting parameter (α), whilst on the contrary, lower α values would be needed to the get less conservative predictions on VA crack growth and, specifically, to better reproduce the overload-induced retardation. It is, therefore, evident that improving the prediction quality for aluminium alloys requires a fundamental modification of the constraint factor conception currently incorporated in the NASGRO SY models.

From Figs 4 and 16, it is obvious that the NASGRO equation is an inadequate description of the da/dN vs. ΔK data for both considered alloys, because the straight line approximation of these data within the Paris regime involved in Eq. (1) is not suitable for materials which, like aluminium alloys, exhibit shear lips. The poor description of the input crack growth data using the NASGRO equation is considered to be the main reason of the inferior predictions on the R-ratio effect under CA loading derived from either model, if coupled with Eq. (1), compared to the predictions based on the discrete da/dN vs. ΔK_{eff} input data.

Also in the case of the programmed VA loading histories, the predictions based on the discrete da/dN vs. ΔK_{eff} input data are superior to those associated with the NASGRO equation, see Fig. 5 against Fig. 13. Specifically, in Fig. 13 the experimental trends due to the presence or absence of the overloads and due to the larger cycles' sequence are more correctly mirrored. Consequently, a closer quantitative agreement between the computed and observed crack growth lives is achieved for the material input data in the discrete form. Unlike in the case of the programmed VA loading, the predictions for the miniFALSTAFF random load sequence based on the input data in the discrete form appear less accurate, i.e. more conservative, than those utilizing the NASGRO equation, as proved by comparing Figs 8 and 14. This finding seems to call to question the utility of the model calibration procedure recommended in the NASGRO manual as it indicates that an analysis option which enables a superior reproducing by the model the

R-ratio effect for CA loading may yield an inferior prediction quality for VA loading.

Of importance to the NASGRO software potential users may be the results shown in Fig. 15, which reveal a failure of the predictions based on the material data picked out automatically from the NASGRO data base. It is obvious, then, that the material parameters from this base should be used with care in that the adequacy of these data must be verified for a specific material through, at least, limited comparisons with the actual test results.

7. Concluding remarks

Predictions of fatigue crack growth under constant amplitude (CA) and variable amplitude (VA) programmed and random loading have been carried out for two aircraft aluminium alloys, namely D16 and 2024-T3 using the strip yield (SY) model available in the NASGRO computer software. Utilizing two different SY models incorporated in NASGRO [constant constraint-loss (CCL) and variable constraint-loss (VCL) model] and two types of the crack growth data description [(NASGRO equation (1) and discrete da/dN vs. ΔK_{eff} data)] enabled altogether four different analysis options. The model performance has been assessed not only through examining the quantitative agreement between the predictions and the fatigue tests results but also by checking if empirical trends due to the change of various loading variables are correctly reproduced in the predictions. The study led to the following more important detailed conclusions:

1. No analysis option enabled to reproduce crack growth retardation observed after application of a single overload cycle. It can be anticipated that the NASGRO SY model will produce unrealistically conservative predictions for load spectra causing large retardation effects.
2. Improving the predictions for CA loading would require using still higher values of the fitting parameter (α), whilst lower α values would be needed to the get less conservative results on VA crack growth. Because α scales the constraint factors incorporated in the models, it is evident that a fundamental modification of the constraint factor conception would be necessary to better the model performance.
3. Though all trends observed in the present experiments are correctly reflected in the predictions, the quantitative correlation between the computed and test results for the VA loading sequences is unsatisfactory and generally worse than that reported in the literature for a more simple semi-empirical crack closure model for crack growth predictions.

4. A satisfactory curve fitting the input crack growth data using the NASGRO equation can be obtained for a range of α values and, hence, it does not guarantee satisfactory prediction results from the SY models, even for CA loading.
5. The poor description of the input crack growth data using the NASGRO equation is considered to be the main reason of inferior crack growth predictions for CA loading derived from either model, if coupled with this equation, compared to the predictions based on the discrete da/dN vs. ΔK_{eff} input data.
6. Though in the case of the programmed VA loading histories the predictions based on the discrete input data were superior to those associated with the NASGRO equation, the reverse was true for the miniFALSTAFF random load sequence. This finding seems to call to question the philosophy of the model calibration procedure recommended in the NASGRO manual, as it indicates that an analysis option which enables a superior reproducing by the model the R-ratio effect for CA loading may yield an inferior prediction quality for VA loading.
7. The VCL model performance was found to be superior compared to the CCL model regarding both the quantitative correlation of the test results and the capability of reproducing the experimental trends.
8. The predictions based solely on the material input data from the NASGRO data base cannot be considered reliable.
9. For CA loading, an insignificant effect of the number of cycles set for one computation step was noted.

The authors would like to acknowledge a partial financial support from the KBN project No. 4 T07C 018 26.

Manuscript received by Editorial Board, June 16, 2005

REFERENCES

[1] Elber W.: Fatigue crack closure under cyclic tension. Engng Fracture Mech., 1970, Vol. 2, pp. 37÷45.

[2] Skorupa M.: Empirical trends and prediction models for fatigue crack growth under variable amplitude loading. ECN-R-96-007, Netherlands Energy Research Foundation ECN, Petten, The Netherlands 1996.

[3] Newman J. C.: A crack closure model for predicting fatigue crack growth under aircraft spectrum loading. Methods and Models for Predicting Fatigue Crack Growth Under Random Loading, ASTM STP 748, 1981, pp. 53÷84.

[4] Skorupa M., Skorupa A., Zachwieja A.: Computer simulation of crack growth in steels under variable amplitude loading using a strip yield model. Mechanika, Kwartalnik AGH, Kraków 1996, Vol. 15, pp. 1÷13.

[5] Chen D. H, Nisitani H.: Analytical and experimental study of crack closure behaviour based on S-shaped unloading curve. Mechanics of Fatigue Crack Closure, ASTM STP 982, 1988, pp. 175÷488.

[6] Daniewicz S. R.: A closed-form small-scale yielding collinear strip yield model from strain hardening materials. Engng Fracture Mech., 1994, Vol. 49(1), pp. 95÷103.

[7] Wang J., Gao J., Guo W., Shen Y.: Effects of Specimen Thickness, Hardening and Crack Closure for the Plastic Strip Model, Theoretical and Applied Fracture Mechanics, 1998; Vol. 29, pp. 49÷57.

[8] Newman J. C.: A nonlinear fracture mechanics approach to the growth of small cracks. Behavior of Short Cracks is Airframe Components, H. Zocher, (ed.), AGARD CP-328, 1983, pp. 6.1÷6.26.

[9] McMaster F. J., Smith D. J.: Predictions of fatigue crack growth in aluminium alloy 2024-T351 using constraint factors. Int. J. Fatigue, 2001, Vol. 23, pp. S93÷S101.

[10] Ten Hoeve H. J., de Koning A. U.: Reference manual of the strip yield module in the NASGRO or ESACRACK software for the prediction of retarded crack growth and residual strength in metal materials. NLR TR 97012 L, National Aerospace Laboratory, The Netherlands, 1997.

[11] Wang G. S., Blom A. F.: A Strip Model for Fatigue Crack Growth Predictions under General Load Conditions. Engng Fracture Mech., 1991, Vol. 40(3), pp. 507÷533.

[12] Skorupa M., Machniewicz T., Skorupa A., Carboni M., Beretta S.: Experimental and theoretical investigation of fatigue crack closure in structural steel. Fatigue 2002, Proc. 8th Int. Fatigue Cong. 2002, Vol. 4/5, pp. 2309÷2316.

[13] NASA: Fatigue crack growth computer program NASGRO Version 3.0 – Reference manual, JSC-22267B, NASA, Lyndon B. Johnson Space Center, Texas 2000.

[14] Ghidini T., Donne C.: Prediction of Fatigue Crack Propagation in Friction Stir Welds, Proc. 4th International Symposium on Friction Stir Welding, 14–16 May 2003, Park City, Utah, USA, on cd-rom edited by the Welding Institute TWI, Abington Hall, UK.

[15] Sander M.: Comparison of fatigue crack growth concepts with respect to interaction effects. In: Nilson F. (ed.): CD-ROM Proceedings of ECF 15, Stockholm 2004.

[16] Newman J. C.: A Crack Opening Stress Equation for Fatigue Crack Growth. Int. J. Fracture, 1984, Vol. 24(3), pp. R131÷R135.

[17] Newman J. C.: FASTRAN II – A fatigue crack growth structural analysis program. NASA TM 104159, Langley Res. Centre, Hampton, VA, U.S.A. 1992.

[18] Schijve J.: Shear lips on fatigue fractures in aluminium sheet material. Engng Fracture Mech., 1981, Vol. 14, pp. 789÷800.

[19] De Koning A. U.: Prediction of fatigue crack growth. NLR TR 87052, National Aerospace Laboratory, The Netherlands, 1987.

[20] Schijve J., Skorupa M., Skorupa A., Machniewicz T., Gruszczyński P.: Fatigue crack growth in the aluminium alloy D16 under constant and variable amplitude loading. Int. J. Fatigue, 2004, Vol. 26, pp. 1÷15.

[21] Misawa H., Schijve J.: Fatigue crack growth in aluminium alloy sheet material under constant-amplitude and simplified flight-simulation loading. Delft University of Technology, Faculty of Aerospace Engineering, Report LR-381, 1983.

[22] Skorupa M.: Load interaction effects during fatigue crack growth under variable amplitude loading. A literature review. Part II: Qualitative interpretation. Fatigue Fract. Engng Mater. Struct., 1999, Vol. 22, pp. 905÷926.

[23] NASA and Southwest Research Institute: NASGRO Fracture Mechanics and Fatigue Crack Growth Analysis Software, Reference Manual, Version 4.02, September 2002.
[24] Schijve J.: Four lectures on fatigue crack growth, Engng Fracture Mech., 1978, Vol. 11(1), pp. 169÷206.
[25] Padmadinata U. H.: Investigation of Crack-Closure Prediction Models for Fatigue in Aluminum Sheet under Flight-Simulation Loading. PhD-thesis, Delft University of Technology, Report LR-6119, 1990.

Przewidywanie wzrostu pęknięć w lotniczych stopach aluminium przy stałoamplitudowych oraz programowanych i losowych zmiennoamplitudowych historiach obciążenia z użyciem modelu pasmowego płynięcia z pakietu NASGRO

Streszczenie

Model pasmowego płynięcia z pakietu NASGRO został zastosowany do prognozowania wzrostu pęknięć zmęczeniowych w dwóch lotniczych stopach aluminium, przy obciążeniach stałoamplitudowych oraz w warunkach programowanych i losowych zmiennoamplitudowych historii obciążeń. Weryfikowane opcje obliczeń uwzględniały użycie dwóch typów modeli pasmowego płynięcia dostępnych w pakiecie NASGRO, a także dwóch sposobów deklarowania wejściowych danych materiałowych. Oceny adekwatności modelu dokonano w oparciu o porównanie wyników przewidywanych i zaobserwowanych w trakcie badań zmęczeniowych. Stwierdzono, że niezadowalająca dokładność symulacji wynika głównie z niewłaściwej koncepcji kalibracji modelu NASGRO do danego materiału.